

Original Research

# AFF3 is a Prognostic Biomarker Correlated with Immune Infiltrates in Triple-Negative Breast Cancer

Jing Chen<sup>1</sup>, Bing Tan<sup>1</sup>, Wei Zhuang<sup>1</sup>, Tenghua Yu<sup>2</sup>, Jianglong Li<sup>2</sup>, Chongwu He<sup>2,\*</sup><sup>1</sup>Nursing Faculty, Nanchang Medical College, 330004 Nanchang, Jiangxi, China<sup>2</sup>Department of Breast Surgery, Jiangxi Cancer Hospital of Nanchang University, 330029 Nanchang, Jiangxi, China\*Correspondence: [361439920088@email.ncu.edu.cn](mailto:361439920088@email.ncu.edu.cn) (Chongwu He)

Academic Editor: Ambrogio Pietro Londero

Submitted: 17 November 2022 Revised: 23 April 2023 Accepted: 28 April 2023 Published: 8 August 2023

## Abstract

**Background:** Triple-negative breast cancer (TNBC) is an aggressive type of breast cancer that cannot be treated with targeted therapies such as endocrine therapy or anti-HER-2 (anti-human epidermal growth factor receptor 2) therapy. In the growth of tumors, *AFF3* (AF4/FMR2 family member 3) plays a critical role. This study aims to examine the prognostic value and immune-related functions of *AFF3* in TNBC. **Methods:** In the Gene Expression Omnibus (GEO) database, differentially expressed genes (DEGs) were identified from three datasets associated with TNBC. Clinicopathologic characteristics, overall survival (OS) data and gene expression data of TNBC patients were acquired from The Cancer Genome Atlas (TCGA). The Kaplan-Meier analyses and proportional hazards model (Cox) regression were used to assess factors associated with OS, including gene expression levels and clinicopathological factors. Gene Ontology, the Kyoto Encyclopedia of Genes and Genomes were performed for the analysis of biological processes associated with DEGs related to TNBC. Gene Set Enrichment Analysis was used to analyze the biological processes associated with *AFF3* in TNBC. Twenty-five paired primary TNBC tumor tissues and adjacent non-tumorous tissues were collected from patients at Jiangxi Cancer Hospital (Nanchang, China). Quantitative real-time polymerase chain reaction (qRT-PCR) and western blotting were performed to assess the mRNA and protein expression of *AFF3* in these samples. Immune cell infiltration status of 152 TNBC samples was analyzed by CIBERSORT algorithm. **Results:** Seventy-five DEGs from three TNBC-related gene expression profiles in GEO database. Based on the L1000 fireworks display (L1000FWD) dataset, five small-molecule drugs which were potentially suitable for treating TNBC patients were obtained. Univariate and multivariate Cox analyses revealed that low *AFF3* expression in TNBC patients was an independent prognostic factor for poor survival. *AFF3* expression was comparatively analyzed in 152 TNBC samples. The CIBERSORT algorithm was used to examine immune cell infiltration in TNBC tumors, which provided useful insights into the interface between the immune system and TNBC. **Conclusions:** In TNBC, low *AFF3* expression might be predictive of poor survival. *AFF3* might provide additional insight into therapeutics in TNBC.

**Keywords:** triple-negative breast cancer; *AFF3*; The Cancer Genome Atlas (TCGA); Gene Expression Omnibus (GEO); biomarker; prognosis; immune cell infiltration

## 1. Introduction

Breast cancer (BC) is the most prevalent malignancy among women worldwide. BC can be categorized into five basic intrinsic or molecular subgroups based on existing molecular and genetic information. There is a spectrum of breast cancer types exists, including luminal A, luminal B, triple-negative/basal-like, HER2 (Human Epidermal Growth Factor Receptor 2)-enriched, and normal-like cancers [1]. The most invasive BC is triple-negative breast cancer (TNBC), accounting for 12–17% of all cases [2], and TNBC is diagnosed in more than 200,000 women annually [3]. TNBC is more aggressive and proliferative and has poorer prognoses and survival rates compared to other breast cancer types [4]. Due to ER (estrogen receptor)-negative, PR (progesterone receptor)-negative, and HER2-negative status, TNBC usually only responds to chemotherapy [5]. Furthermore, the prognosis of the patient with TNBC is not always favorable. Therefore, there is an urgent

need to identify prognostic biomarkers to develop efficient therapeutic strategies for patients with TNBC.

The AFF (AF4/FMR2) protein family includes four members. The expression of AFF1/2/3/ is localized in the nucleus. *AFF3* (AF4/FMR2 family member 3) was initially thought to be a lymphoid gene. It may function in transcriptional control. Additionally, *AFF3* is reported to mediate tamoxifen resistance in BC [6]. However, the role and mechanisms of *AFF3* in TNBC have not been elucidated.

In this study, differentially expressed genes (DEGs) were identified using three TNBC datasets in the Gene Expression Omnibus (GEO) database. Subsequently, univariate and multivariate proportional hazards model (Cox) analyses revealed that low *AFF3* expression in TNBC is able to predict survival of TNBC as an independent prognostic factor.

Furthermore, DEGs were obtained by comparison between TNBC samples according to the levels of *AFF3* ex-



pression from The Cancer Genome Atlas (TCGA) data. Using CIBERSORT, we profiled immune cell types in TNBC tumors to gain insight into the immune system's interface. The findings of this study indicated *AFF3* is a potential indicator for treatment targets in TNBC patients.

## 2. Materials and Methods

### 2.1 Tissues

The primary tumor (T) and adjacent non-tumorous (N) tissue samples were obtained from 25 patients with TNBC undergoing surgery at Jiangxi Cancer Hospital (Nanchang, China). All paired tumor and normal tissue samples were independently identified by two pathologists. These samples were examined by quantitative real-time polymerase chain reaction (qRT-PCR) and western blotting analyses. All samples were stored at  $-80^{\circ}\text{C}$  until analysis. The tissue specimens were collected with the consent of patients from July 2019 to September 2020. The Ethics Committee of the Jiangxi Cancer Hospital approved the study design. All patients signed an informed consent form.

### 2.2 Data Source

Three gene microarray datasets (GSE38959 [7], GSE62931 [8] and GSE64790 [9]) of expression profiles of TNBC tissues or TNBC cells and non-TNBC samples or healthy mammary ductal cells or healthy breast tissues were obtained from the GEO database (<https://www.ncbi.nlm.nih.gov/geo/>). High-throughput RNA sequencing data and clinicopathological data of breast cancer patients were downloaded from TCGA [10]. We confirmed the ER, PR and HER2 expression status of all breast cancer patients in TCGA based on the immunohistochemical (IHC). Information on patients with TNBC was extracted according to the classification system proposed by Voduc *et al.* [11]. These patients were enrolled in the TCGA-TNBC cohort.

### 2.3 Screening for DEGs

The data were divided into TNBC and non-TNBC subsets. DEGs between the TNBC and non-TNBC samples were filtered by the Limma package in R (version 3.5.0, R Foundation for Statistical Computing, Vienna, Austria). To screen TNBC-related DEGs, the following criteria were used: false discovery rate (FDR)  $< 0.05$  and  $|\log_2 \text{fold change (FC)}| > 1.5$ . The VennDiagram package in R was used to overlap DEGs obtained from three GEO datasets. Finally, the overlapping genes were defined as DEGs.

### 2.4 Gene Ontology (GO) and Kyoto Encyclopedia of Genes and Genomes (KEGG) Enrichment Analyses

To clarify the biological processes in which *AFF3* and all DEGs, GO [12] and KEGG [13] analyses were performed using the clusterProfiler R package. Significant DEGs were identified based on the following criteria:  $p < 0.05$  and FDR  $q$ -values  $< 0.05$ .

### 2.5 Gene Set Enrichment Analysis (GSEA)

GSEA is a computational method that determines whether an a priori defined set of genes shows statistically significant, concordant differences between two biological states. In order to analyze correlations among all DEGs, clusterProfiler package was used to perform GSEA [14,15].

GSEA firstly generated an ordered list of all DEGs according to their correlation with *AFF3* expression and gene set permutations were performed 1000 times for each analysis. The criteria for significant correlations were as follows:  $p < 0.05$ ; FDR  $q$ -values  $< 0.25$ .

### 2.6 Identification of Potential Small-Molecule Drugs

Based on the TNBC-related DEGs, the L1000 fire-works display (L1000FWD) database [16] was utilized to predict prospective drugs that could attenuate or enhance the biological status of TNBC. The DEGs were submitted to the L1000FWD database for potential small-molecular drugs for TNBC. The closer the similarity score is to  $-1$ , the higher the efficacy of the drug against TNBC.

### 2.7 Survival Analysis

Survival analysis was conducted using survival and survminer packages. The survival duration of 152 patients with TNBC for whom detailed survival data were available was 0–9.61 years. The Kaplan–Meier method was used to draw the survival curve. Statistical significance was assessed by the log-rank test and  $p < 0.05$  was considered significant.

### 2.8 Cox Regression Analysis

To further determine the effect of gene expression and clinical characteristics in TNBC patients, univariate Cox regression analysis was used to calculate the association between gene expression and clinical characteristics and patient's overall survival (OS) in TCGA-TNBC cohort. Afterwards, a multivariate analysis was used to assess the independent prognostic factor for TNBC patient survival. The survival package in R was used to perform univariate and multivariate Cox regression.

### 2.9 Evaluation of the Tumor Microenvironment (TME) and Tumor-Infiltrated Immune Cells (TICs)

The CIBERSORT algorithm [17], which can analyze the composition of immune cells in samples based on RNA high-throughput sequencing data, was applied to assess tumor-infiltrating immune cell (TICs) in tumor tissues of TCGA-TNBC cohort. The permutation (perm) was set at 1000 to obtain more stable results.

### 2.10 Western Blotting Analysis

Radioimmunoprecipitation lysis buffer was used to lyse TNBC samples and adjacent non-tumorous tissues. The supernatant was collected after centrifugation for 10 min at 12,000 g. The bicinchoninic acid (BCA) protein

**Table 1. The information of datasets selected from the Gene Expression Omnibus (GEO) database.**

Accession number	Platform	Sample type and number	Experiment type
GSE38959	GPL4133	TNBC cells (30) normal mammary ductal cells (13)	Expression profiling by array
GSE62931	GPL15048	TNBC samples (47) non-TNBC (ER+/PR+) samples (53)	Expression profiling by array
GSE64790	GPL19612	TNBC tissue (3) matched normal breast tissues (3)	Expression profiling by array Non-coding RNA profiling by array

TNBC, Triple-negative breast cancer; ER+, estrogen receptor – positive; PR+, progesterone receptor – positive.

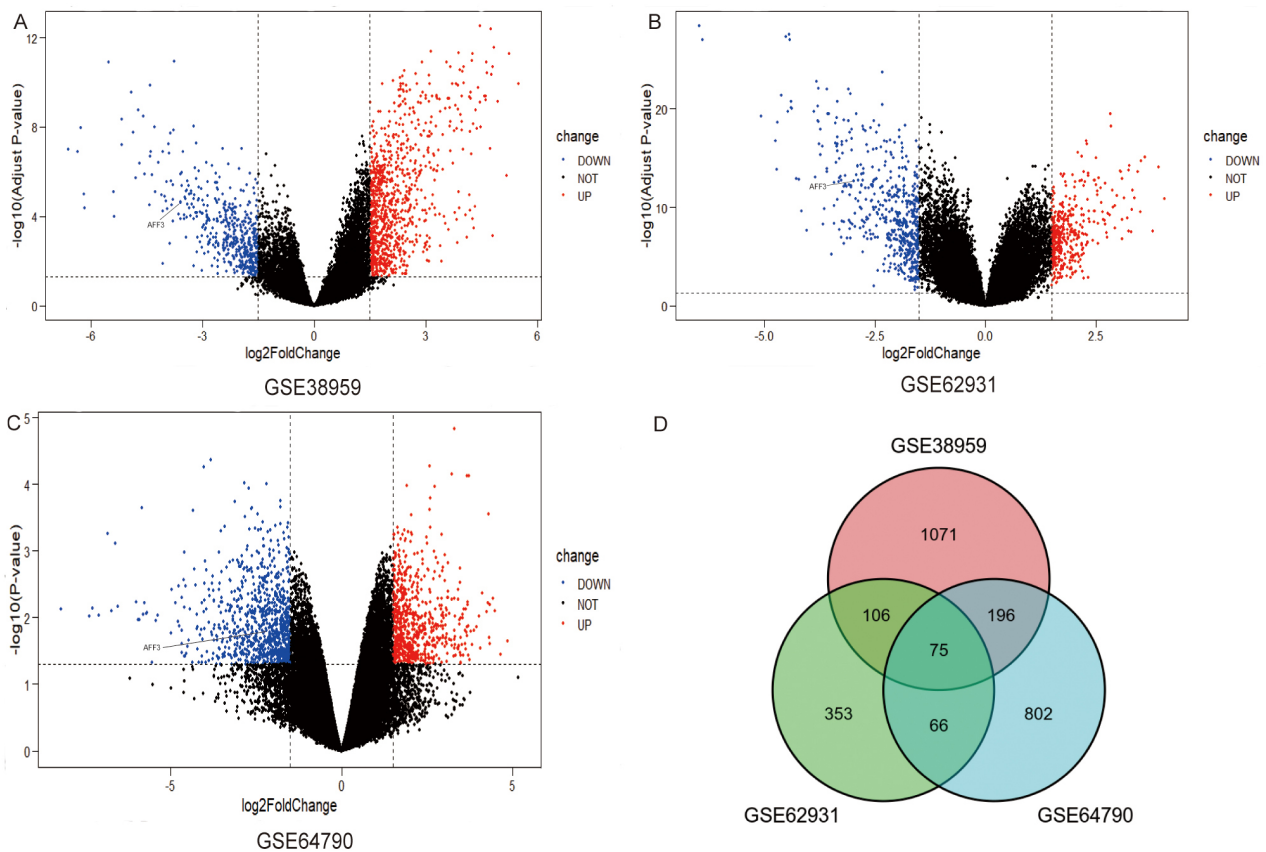


**Fig. 1. Identification of differentially expressed genes (DEGs) in triple-negative breast cancer (TNBC).** (A–C) Volcano map of three genes expression profiles in GEO datasets, GSE38959 (A), GSE62931 (B), and GSE64790 (C). Red and blue colors indicate upregulated and downregulated genes in tumor tissues, respectively. (D) Venn diagram showing the common DEGs in three datasets.

quantification kit (Beijing Cwbiotech Co., Ltd., Beijing, China) measured the total protein content. After mixing the protein with the loading buffer, it was boiled for 10 min in a water bath. Protein lysates (20  $\mu$ g) was separated by 10% sodium dodecyl sulfate polyacrylamide gel electrophoresis (SDS-PAGE) and transferred onto a polyvinyl difluoride (PVDF) membrane (10600023, GE Healthcare Life Sciences, Woburn, MA, USA). Nonspecific binding protein on PVDF was blocked by 10% Bovine Serum Albumin (BSA, GC305006, Servicebio, Wuhan, Hubei, China). Then, the membranes were incubated with antibodies against *AFF3* (1:1000, ab106231) and  $\beta$ -tubulin (1:500; ab6040) (Abcam, Cambridge, MA, USA). After washing the PVDF membrane several times, the PVDF membrane was incu-

bated with a corresponding secondary antibody (1:4000, ab6721). After washing the PVDF membrane several times again, bands on the PVDF membrane were detected on a Bio-Rad ChemiDoc XRS system.

### 2.11 Reverse Transcription and Quantitative Real-Time PCR (qRT-PCR)

Total RNA was extracted and reverse-transcribed into complementary DNA (cDNA) using the all-in-one first-strand cDNA synthesis super mix kit (TransGen Biotech, Beijing, China). qRT-PCR analysis was performed using the fast green qRT-PCR supermix (TransGen Biotech, Beijing, China). All samples were divided into tumor tissue (T) or non-tumorous tissue (N) to

**Table 2. The five most similar small-molecule drugs obtained from L1000FWD database.**

Drug	Similarity score	<i>p</i> -value	Adjusted <i>p</i> -value	Z-score	Combined score
Idarubicin	-0.4754	$4.92 \times 10^{-33}$	$9.29 \times 10^{-29}$	1.77	-57.17
Teniposide	-0.4754	$3.93 \times 10^{-33}$	$9.29 \times 10^{-29}$	1.76	-56.89
Homosalate	-0.4754	$6.51 \times 10^{-33}$	$9.29 \times 10^{-29}$	1.68	-54.20
Palbociclib	-0.4426	$1.05 \times 10^{-30}$	$7.48 \times 10^{-27}$	1.72	-51.47
Tremulacin	-0.4426	$3.18 \times 10^{-30}$	$1.94 \times 10^{-26}$	1.74	-51.36

L1000FWD, L1000 fireworks display.

**Table 3. Multivariate Cox regression analysis of correlation of overall survival with clinicopathological characteristics and gene expression in TCGA-TNBC cohort.**

Clinicopathologic variable or gene expression	Hazard ratio (95% confidence interval)	<i>p</i> -value
<i>NUF2</i> (high vs. low)	0.53 (0.07–4.07)	0.541
<i>TPX2</i> (high vs. low)	0.8 (0.06–11.25)	0.866
<i>BUB1</i> (high vs. low)	2.47 (0.19–32.2)	0.491
<i>EZH2</i> (high vs. low)	0.4 (0.12–1.37)	0.144
<i>ASPM</i> (high vs. low)	1.07 (0.13–8.82)	0.947
<i>EXO1</i> (high vs. low)	0.53 (0.07–4.04)	0.540
<i>DEPDC1</i> (high vs. low)	0.51 (0.04–5.75)	0.583
<i>AFF3</i> (high vs. low)	0.22 (0.07–0.72)	<b>0.012</b>
<i>HI-1</i> (high vs. low)	0.75 (0.26–2.14)	0.587
<i>PSAT1</i> (high vs. low)	0.29 (0.06–1.29)	0.104
<i>NDC80</i> (high vs. low)	0.8 (0.2–3.25)	0.755
<i>CENPF</i> (high vs. low)	1.05 (0.19–5.87)	0.960
<i>KIF18B</i> (high vs. low)	3.3 (0.55–19.88)	0.193
Race (non-white vs. white)	0.61 (0.21–1.79)	0.369
N stage (N2 + N3 vs. N0 + N1)	1.12 (0.11–11.2)	0.921
T stage (T3 + T4 vs. T1 + T2)	1.59 (0.27–9.37)	0.607

Bold indicates that *AFF3* is an independent risk factors for overall survival in triple-negative breast cancer patients.

detect the mRNA expression of *AFF3*. The  $2^{-\Delta\Delta CT}$  method was used to calculated relative gene expression. The corresponding primer sequences were as follows: *AFF3*: 5'-ACTCAACAGGATGATGGC-3' (forward) and 5'-TGCCTAAAGTGTCTGGATC-3' (reverse); *glyceraldehyde-3-phosphate dehydrogenase (GADPH)*: 5'-GGTGAAGGTCGGAGTCAACG-3' (forward) and 5'-CAAAGTTGTCATGGATGHACC-3' (reverse).

### 2.12 Statistical Analysis

All statistical analyses were performed using the R software (version 3.5.0, the Vienna University of Economics and Business, Vienna, Austria). Clinicopathological and immune infiltration data between different groups were tested by Wilcoxon test. The Correlation between *AFF3* expression and TICs was examined using Spearman correlation analysis. All statistical tests were two-sided, and the level of significance was set at  $p < 0.05$ .

## 3. Results

### 3.1 Identification of DEGs in TNBC

As shown in Table 1, we selected three GEO datasets for analysis. The number of upregulated and downregulated

genes in different datasets were as follows: GSE38959, 939 upregulated genes and 509 downregulated genes (Fig. 1A); GSE62931, 356 upregulated genes and 483 downregulated genes (Fig. 1B); GSE64790, 509 upregulated genes and 630 downregulated genes (Fig. 1C). Fig. 1D shows a Venn diagram with 75 overlapping DEGs, comprising 38 upregulated and 37 downregulated genes (**Supplementary Table 1**).

### 3.2 Functional Enrichment Analysis of DEGs

GO and KEGG functional enrichment analyses were performed with ClusterProfiler to examine the functional implications of 75 DEGs between TNBC and non-TNBC samples. The biological process (BP) included mitotic nuclear division, nuclear division, organelle fission, chromosome segregation and kinetochore organization. Cellular components (CC) were condensed chromosome kinetochore, condensed chromosome, condensed nuclear chromosome kinetochore, condensed chromosome, centromeric region, kinetochore; KEGG enrichment suggested progesterone-mediated oocyte maturation, cell cycle, and oocyte meiosis (Fig. 2, **Supplementary Table 2**).

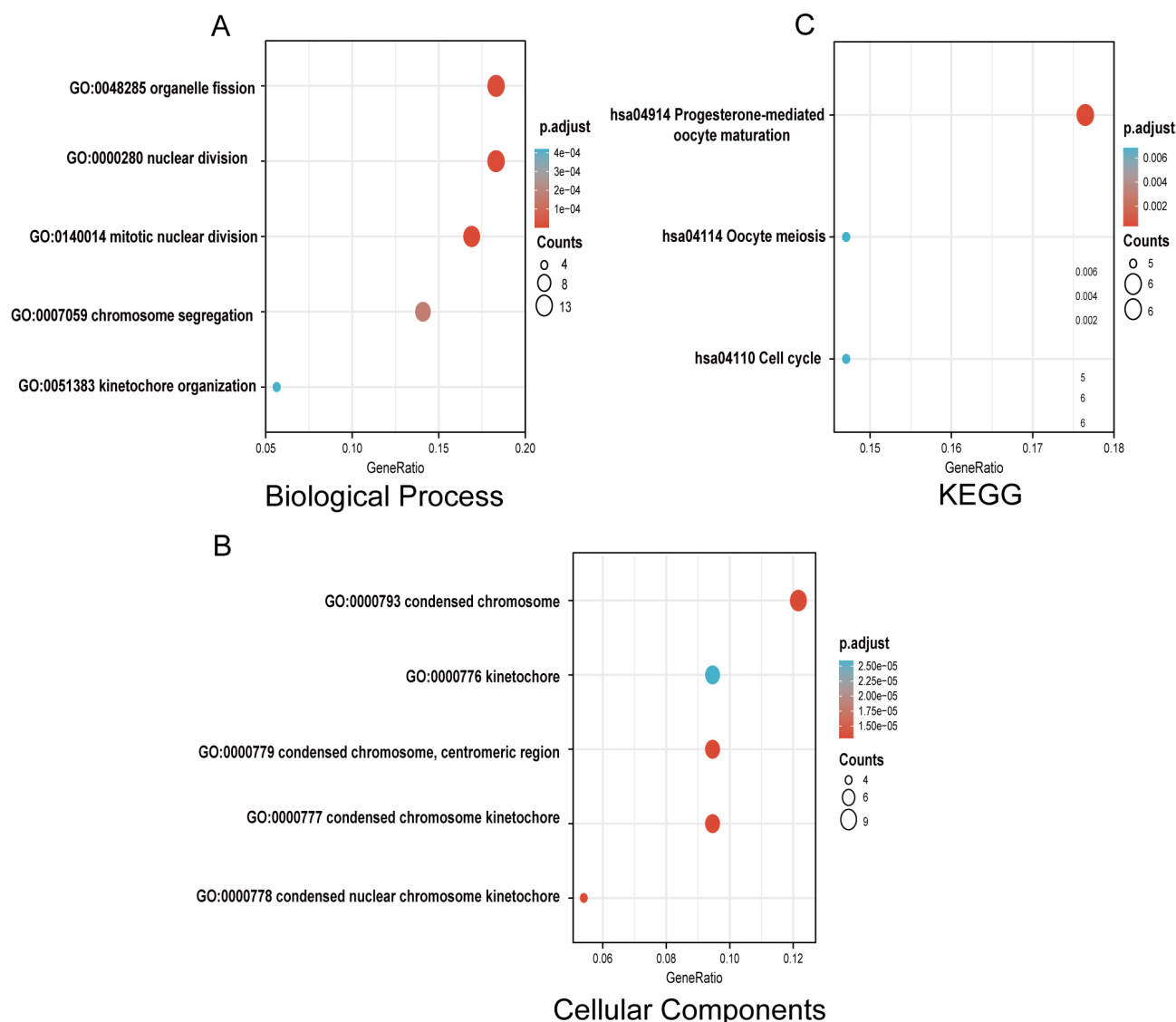


**Fig. 2. Gene Ontology (GO) and Kyoto Encyclopedia of Genes and Genomes (KEGG) enrichment analyses of DEGs between TNBC and non-TNBC tissues.** (A) Enriched GO terms in the “biological process” category. (B) Enriched GO terms in the “Cellular Components” category. (C) KEGG pathway annotations. The size of the circle represents the number of genes contained in a category. The higher the number of genes, the larger the circle. The color represents the adjusted  $p$ -value in enrichment analysis. The smaller the  $p$ -value, the higher the red color intensity. The larger the  $p$ -value, the higher the blue color intensity.

### 3.3 Small-Molecule Drugs

To screen for drugs for TNBC treatment, upregulated and downregulated DEGs were separately uploaded into the L1000FWD database. Small-molecules with anticancer effects on TNBC progression were selected with a similarity score of zero and an adjusted  $p$ -value of 0.01. The five most similar small-molecule drugs were idarubicin, teniposide, homosalate, palbociclib, and tremulacin (Table 2).

### 3.4 Univariate and Multivariate Analyses

The correlation between gene expression and clinical characteristics in TCGA-TNBC dataset was examined.

Gene expression matrices and clinicopathological data of 152 TNBC patients were obtained. Univariate Cox regression analysis revealed that 13 DEGs (*NUF2*, *TPX2*, *BUB1*, *EZH2*, *ASPM*, *EXO1*, *DEPDC1*, *AFF3*, *H1-1*, *PSAT1*, *NDC80*, *CENPF*, and *KIF18B*), race, T stage, and N stage were correlated with prognosis of TNBC patients ( $p < 0.1$  was considered statistically significant, **Supplementary Table 3**). Multivariate analysis revealed that among the 13 genes and 3 clinicopathological variables mentioned above, only *AFF3* downregulation (hazard ratio (HR): 0.22; 95% confidence interval (CI): 0.07–0.72;  $p = 0.012$ ) was an independent risk factor for OS in patients with TNBC (Table 3).

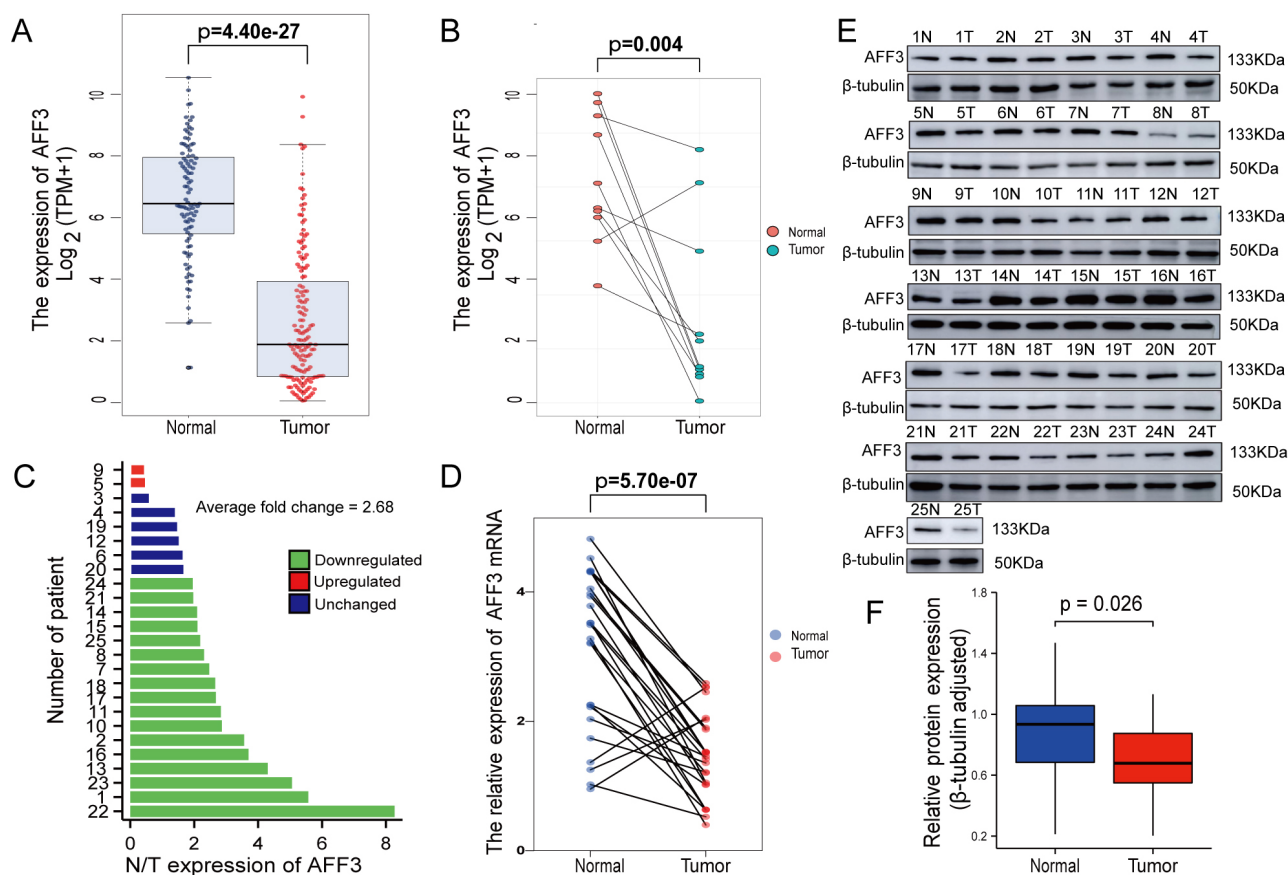


**Fig. 3. Expression of *AFF3* in TNBC and non-tumorous tissues.** (A) The relative mRNA expression of *AFF3* in 152 TNBC tissues and 99 non-tumorous tissues in TCGA dataset. Significant differences between the two groups were evaluated using the Wilcoxon rank sum test. (B) The relative mRNA expression of *AFF3* in 10 TNBC tissues and paired-adjacent tissues from TCGA dataset. Significant differences between the two groups were analyzed using the Wilcoxon signed-rank test. (C) The *AFF3* mRNA levels in 25 paired samples of TNBC are represented as a histogram. N/T expression value  $\geq 2$  suggests a significantly lower expression, which  $\leq 1/2$  is a significantly higher expression, and values between  $1/2$  and  $2$  show no significant change. N, non-tumorous tissue; T, tumor tissue. (D) The *AFF3* mRNA expression levels in paired N and T from 25 TNBC patients. Significant differences between the two groups were evaluated using the Wilcoxon signed-rank test. (E) The *AFF3* protein levels in 25 paired N and T.  $\beta$ -tubulin was an internal control. (F) The quantified *AFF3* protein level in 25 paired N and T. Significant differences between the two groups were evaluated using the Wilcoxon signed-rank test.

### 3.5 Downregulated *AFF3* Expression in the TCGA-TNBC Cohort

The transcription levels of *AFF3* in TCGA-TNBC cohort were analyzed. The expression of *AFF3* in TNBC tumor tissues was significantly lower than that in healthy mammary tissues ( $p = 4.40 \times 10^{-27}$ , Fig. 3A). Compared with those in the paired non-tumorous tissues, the *AFF3* mRNA levels were downregulated in the TNBC tumor tissues. Next, the mRNA and protein expression levels of *AFF3* in 25 paired samples of TNBC collected from patients at Jiangxi Cancer Hospital were examined using qRT-PCR (Fig. 3C,D) and western blotting (Fig. 3E). Compared with those in the non-tumorous tissues (N), the mRNA (with an average fold change of 2.68, Fig. 3C) and protein levels (Fig. 3F) of *AFF3* were downregulated in the TNBC tumor tissues (T).

### 3.6 Correlation between Clinical Characteristics and *AFF3* mRNA Expression Level in TCGA-TNBC Cohort Patients

Next, the correlation between clinicopathological and *AFF3* expression was further investigated in TCGA-TNBC cohort. All patients in the TCGA-TNBC cohort were categorized into *AFF3*-high and *AFF3*-low groups, based on the median *AFF3* expression levels. The *AFF3* mRNA expression level was significantly correlated with T stage ( $p = 0.025$ , Fig. 4A), N stage ( $p = 0.008$ , Fig. 4B), pathologic stage ( $p = 0.046$ , Fig. 4D), race ( $p = 0.023$ , Fig. 4E). In TCGA-TNBC cohort, the median OS in the *AFF3*-high group was higher than that in the *AFF3*-low group ( $p = 0.023$ , Fig. 4F).

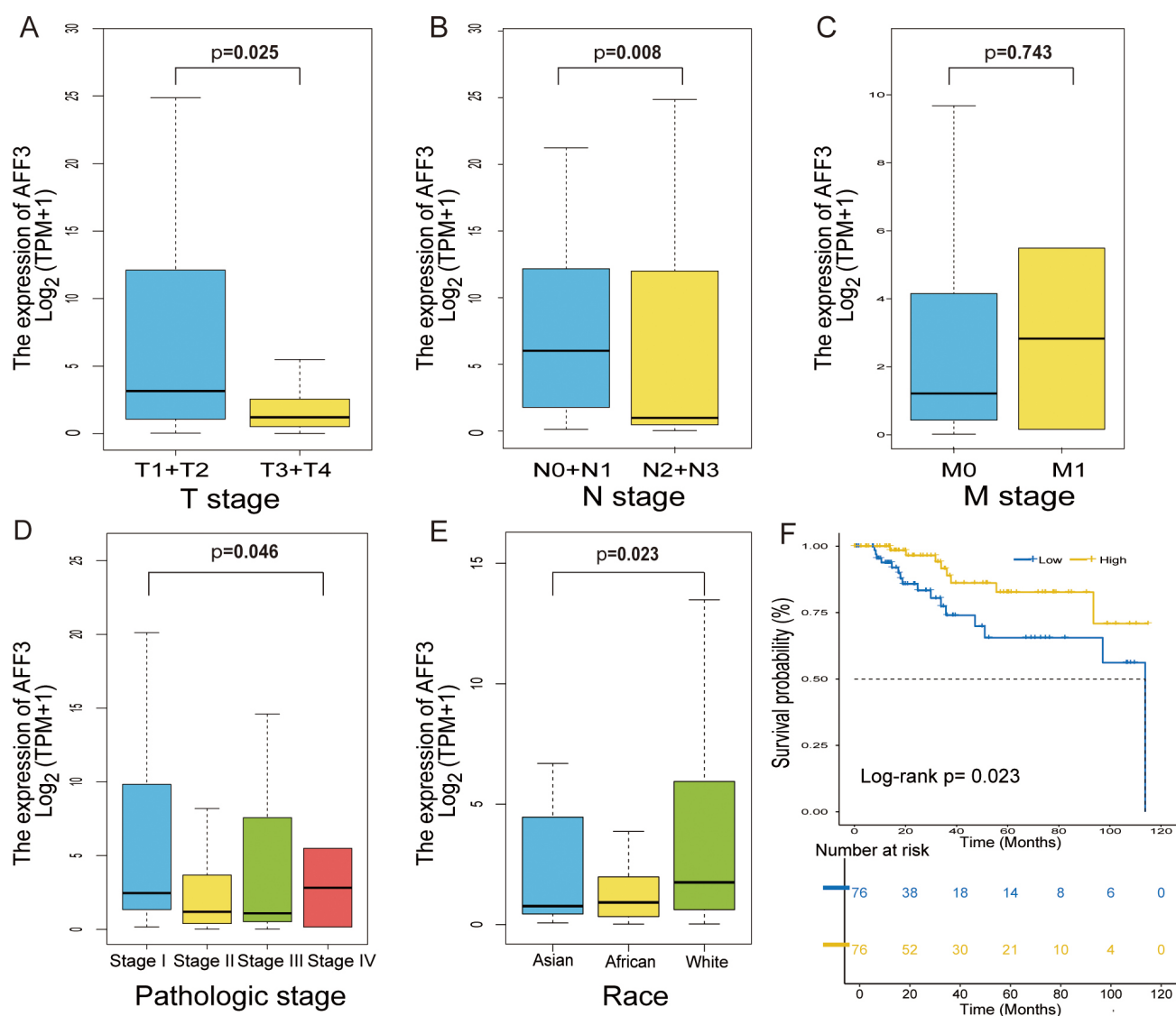


**Fig. 4. Correlation of *AFF3* mRNA expression with clinicopathological characteristics.** (A–C) The correlation of *AFF3* mRNA expression with T stage (A), N stage (B), and M stage (C). Significant differences between the two groups examined using the Wilcoxon Mann-Whitney test. (D,E) The correlation of *AFF3* mRNA expression with pathologic stage (D) and race (E). Significant differences between multiple groups were examined using the Kruskal-Wallis rank sum test. (F) Survival analysis of patients with TNBC in the *AFF3*-high and *AFF3*-low groups in TCGA-TNBC cohort. Significant differences between multiple groups were examined using the log-rank test. The number of samples as follows: T1 + T2: 133, T3 + T4: 19; N0 + N1: 131, N2 + N3: 15; M0: 129, M1: 2; stage I: 27, stage II: 96, stage III: 24, stage IV: 2; Asian: 8, White: 84, African: 53.

### 3.7 DEGs between *AFF3*-High and *AFF3*-Low Groups in TCGA-TNBC Cohort

To further investigate the function of *AFF3*, the DEGs between *AFF3*-high and *AFF3*-low groups were examined using the Limma package. The criteria for selecting DEGs were as follows:  $FDR < 0.05$  and  $|\log_2 FC| \geq 2$ . In total, 182 up-regulated genes, and 67 down-regulated genes were obtained. The correlation between the expression of DEGs and samples was shown using a heatmap (Fig. 5A, **Supplementary Table 4**). GO and KEGG enrichment analyses revealed that DEGs were significantly correlated with some

biological processes and signaling pathways, such as cornification, cornified envelopes, and oxidoreductase activity (Fig. 5B,C, **Supplementary Table 5**). Cytochrome P450 enriched steroid hormone biosynthesis, drug metabolism, and xenobiotic metabolism were annotated in KEGG enrichment analysis (Fig. 5D, **Supplementary Table 5**).

### 3.8 GSEA Revealed Some *AFF3*-Related Signaling Pathways

GSEA was performed to investigate the differential activation of *AFF3*-related signaling pathways in TNBC. GSEA identified some critical signaling path-

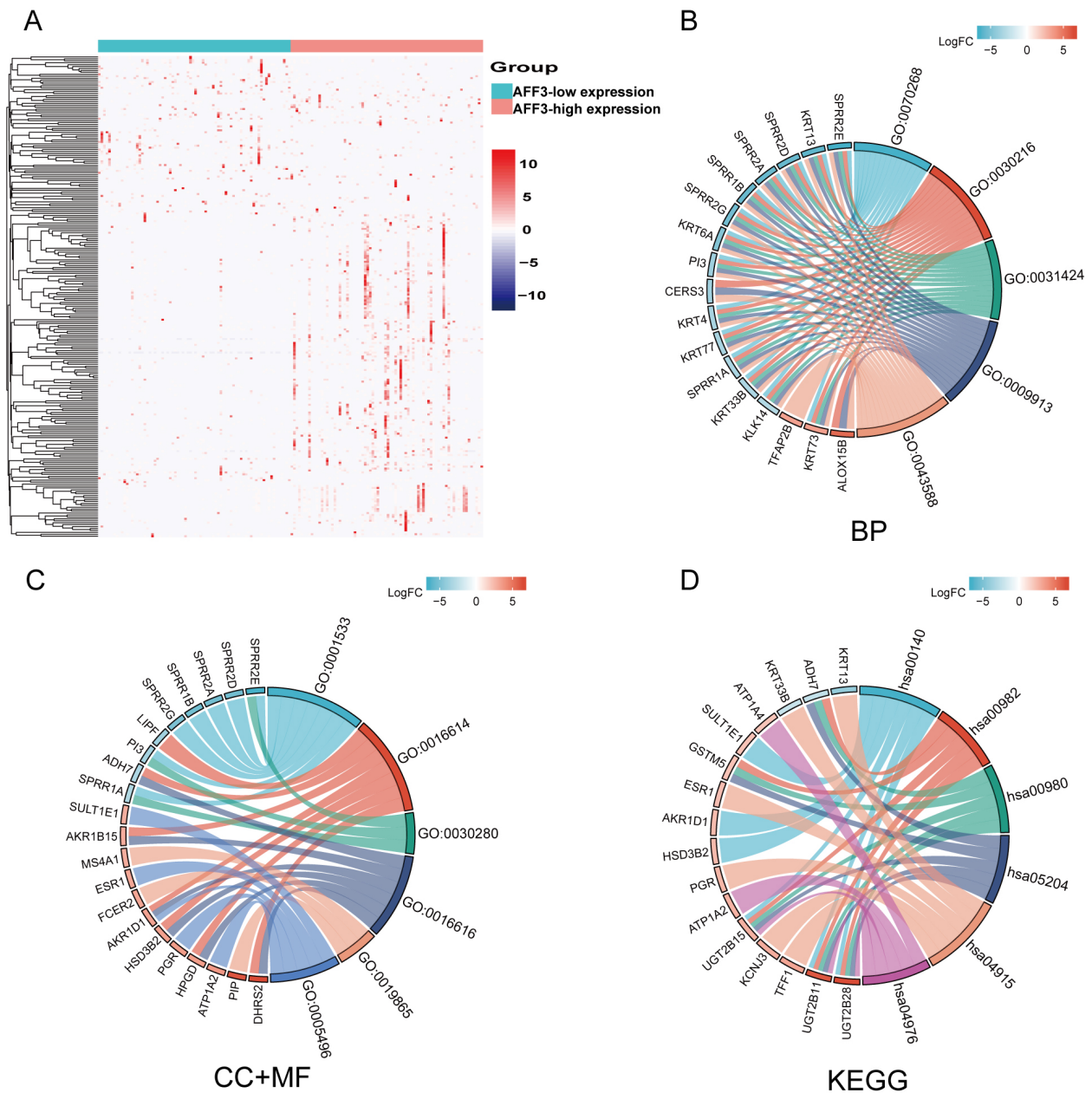


**Fig. 5. GO/KEGG enrichment analysis for DEGs in the *AFF3*-high and *AFF3*-low groups.** (A) Heatmap of DEGs between *AFF3*-high and *AFF3*-low groups. The row of the heatmap represents the gene symbol of the 249 DEGs and the column represents ID number of the samples in TCGA-TNBC cohort. Gene symbols and identification numbers are not shown in the graph. (B) Enriched GO terms in the “biological process” category. (C) Enriched GO terms in the “cellular component” and “molecular function” category. (D) KEGG pathway annotations. Only some notable and leading gene sets are displayed in the graph.

ways in MSigDB collection (c2.cp.v7.2.symbols.gmt and c7.all.v7.2.symbols.gmt). Based on the normalized enrichment score (NES) and *p*-values, some significant signaling pathways are shown (Fig. 6 and **Supplementary Table 6**). For the C2 (one of the human collections of the molecular signatures database) collection, neuroactive ligand receptor interaction, steroid hormone biosynthesis and phase II conjugation of compounds (Fig. 6A, **Supplementary Table 6**) were enriched in *AFF3*-high group. Meanwhile, the

formation of the cornified envelope, keratinization, translation, respiratory electron transport, and complex I biogenesis were enriched in *AFF3*-low group (Fig. 6B, **Supplementary Table 6**). For the C7 collection, some different immune-related signaling pathways were enriched in *AFF3*-high group (Fig. 6C, **Supplementary Table 7**) or *AFF3*-low group (Fig. 6D, **Supplementary Table 7**). These results further suggested that *AFF3* had an important role in the immune microenvironment of TNBC.

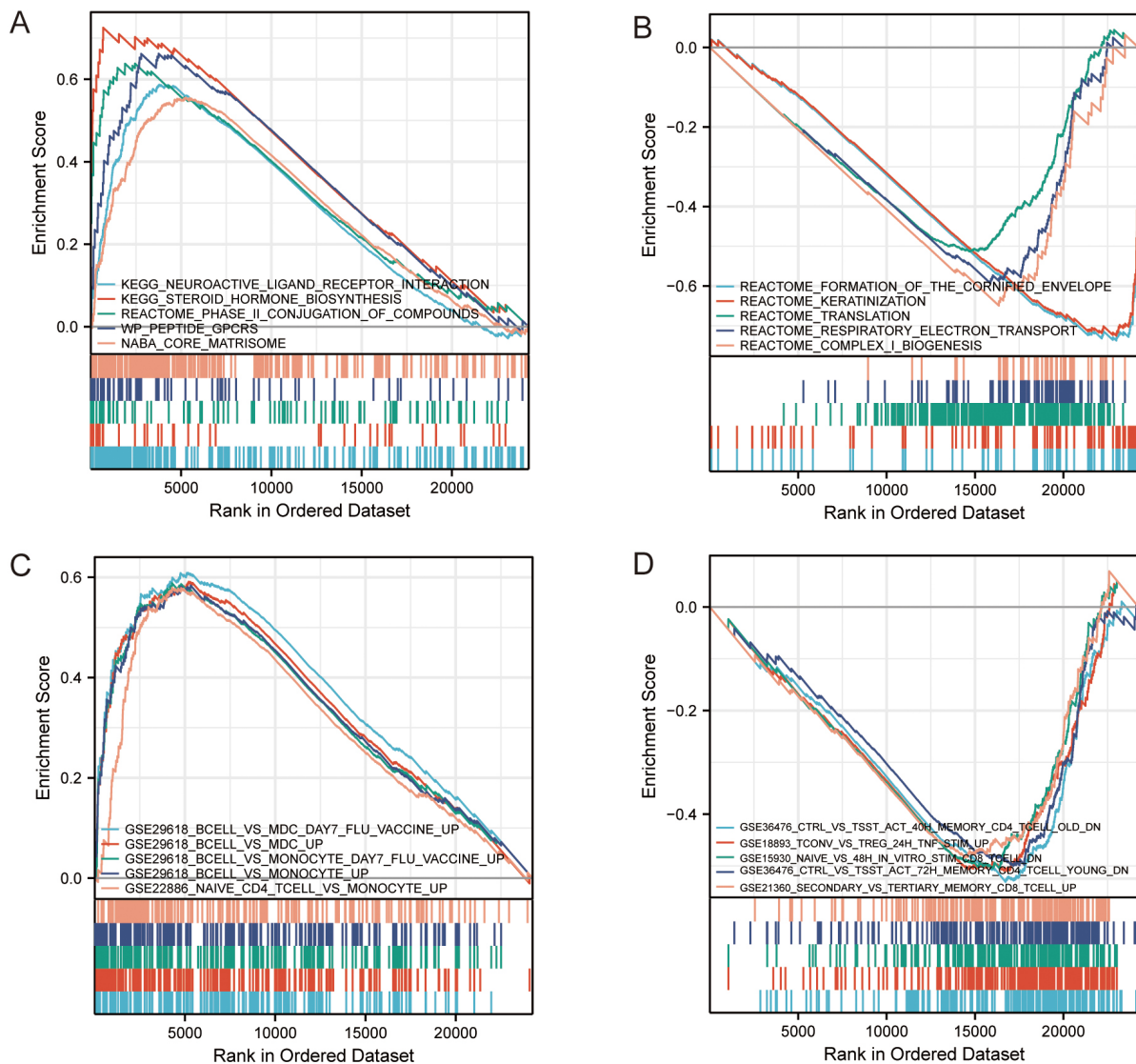


**Fig. 6. GSEA identifies *AFF3*-related signaling pathways.** (A,B) Enriched signaling pathways in the C2 collection in the *AFF3*-high (A) or in *AFF3*-low expression groups (B). (C,D) Enriched signaling pathways in the C7 collection in *AFF3*-high (C) and *AFF3*-low groups (D). GSEA, Gene Set Enrichment Analysis.

### 3.9 Assessment of the Immune Microenvironment in TNBC

GSEA revealed that *AFF3* may be involved in the immune function in TNBC. Next, the distribution of immune cells in TNBC was analyzed with CIBERSORT algorithm. M0, M1, and M2 macrophage subsets accounted for most of the infiltrating immune cells (Fig. 7A). Violin plots were used to compare immunity subset distributions between the *AFF3*-low and *AFF3*-high groups (Fig. 7B). The proportions of naive B cells, neutrophils, and M2 (a subtype of macrophage) macrophages were significantly different between the *AFF3*-low and *AFF3*-high groups (Fig. 7B). The proportions of naive B cells, mast cells resting and T cells CD4 (Cluster of differentiation 4) memory resting were positively correlated with *AFF3* expression (Fig. 7C–E). In contrast, the proportions of neutrophils and follicular helper T cells were negatively correlated with *AFF3* expression.

Therefore, the level of *AFF3* regulates the proportion of TICs and immune activity in TME (Tumor microenvironment).

## 4. Discussion

This study mined the public bioinformatics databases (GEO and TCGA) and tested tissue samples. *AFF3* expression in the tumor tissues was lower than that in the healthy mammary tissue. The *AFF3* mRNA expression level was negatively correlated with T stage, N stage, and was positively correlated with survival status. The downregulation of *AFF3* was an independent poor prognostic factor for TNBC. The underlying mechanisms of *AFF3* may involve cellular hormone metabolic process, humoral immune response, and the regulation of trans-synaptic signaling.

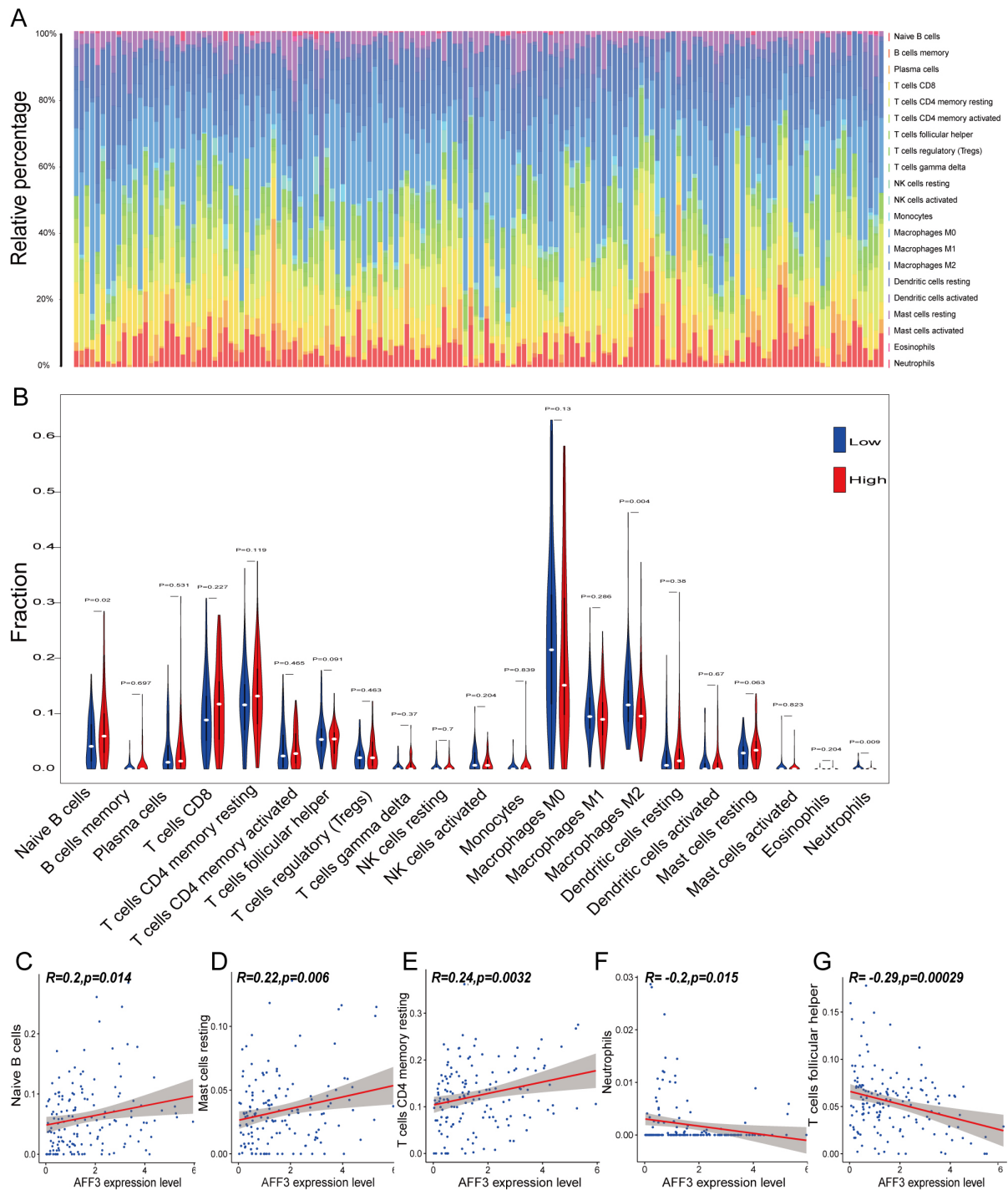


**Fig. 7. Correlation of tumor-infiltrating immune cell (TIC) proportion with *AFF3* expression.** (A) Bar plot shows the distribution of TICs in each tumor sample in TCGA-TNBC cohort. Column are the ID numbers of the samples, which are not shown in the plot. (B) The violin plot shows the distribution of TICs between the *AFF3*-high and *AFF3*-low groups in TCGA-TNBC cohort. (C–G) The scatter plot shows the distribution of the 5 TICs that were significantly correlated with *AFF3* expression.

Previous research reported *AFF3* acted as a mediator of oncogenic effects during transcription and RNA splicing [18]. A previous study reported that *AFF3* may play a role in promoting tumor progression in breast cancer [19], but this study did not distinguish between the subtypes of

BC. Shi *et al.* [6] reported that tamoxifen-resistant tumors exhibited upregulated expression of *AFF3*, which activated the ER signaling pathway. Chen *et al.* [20] reported that *AFF3* was significantly correlated with the prognosis of TNBC (HR = 0.29, 95% CI: 0.10–0.86,  $p = 0.0263$ ), which

was consistent with the results of this study. This study is the first to investigate the expression and biological function of *AFF3* in TNBC.

This study arrived at the following conclusions: (1) univariate and multivariate analyses revealed downregulated *AFF3* expression was an independent poor prognostic factor for TNBC; (2) clinical and pathological characteristics were correlated with the downregulated expression of *AFF3* mRNA; (3) Downregulated *AFF3* expression was also correlated with the distribution of immune cell subsets, such as M2 macrophages, naïve B cells, and neutrophils.

Previous studies have demonstrated that immune cell infiltration is involved in various pathological processes in TNBC, such as tumorigenesis, tumor progression, and therapy response. This study examined the role of *AFF3* in immune cell infiltration. The levels of M2 macrophages, naïve B cells, and neutrophils were significantly upregulated in the *AFF3*-low group. M2 macrophage polarization may be involved in tumor progression as it suppresses effective anti-tumor immunity and decreases the effectiveness of immunotherapy [21]. By interfering with the distribution of TIC in TME, patients with downregulated *AFF3* expression may benefit from immunotherapy.

Additionally, five potential small-molecule drugs for TNBC patients were identified using the L1000FWD dataset. Idarubicin, an anthracycline antibiotic, is used to treat various cancers, such as acute leukemia, malignant lymphomas, and several solid tumors [22,23]. Teniposide, an inhibitor of DNA topoisomerase II, induces innate immune activation in tumor cells and activates antitumor T-cells *in vitro* and *in vivo* [23]. Homosalate, which belongs to the salicylate family of organic compounds, is a salicylic acid incorporated into 3,3,5-trimethylcyclohexanol, a derivative of cyclohexanol. Previous studies have reported that homosalate regulates BC development [24]. Palbociclib is a selective CDK4 (cyclin dependent kinase 4) and CDK6 (cyclin dependent kinase 6) inhibitor. According to experiments in TNBC cell lines, the luminal-AR subtype [25], a subgroup of TNBC, is more sensitive to CDK4/6 inhibition than the other subtypes [26]. Therefore, CDK4/6 inhibitors should be selected according to the patient's subgroup within TNBC [27]. Tremulation was glycoside-derived and showed different levels of inhibition of prostaglandin E2 (PGE2) release [28]. Several recent studies have demonstrated that PGE2 is linked to the progression and treatment of breast cancer in recent years [29,30].

This study performed bioinformatics mining and collected 25 paired tumor and non-tumorous from patients with TNBC. More patient samples and clinicopathological information, including disease free survival and OS, should be collected verify the accuracy of the results of this study. This study did not experimentally validate the bioinformatics results *in vivo* or *in vitro*. Further experiments are needed to verify the functions of *AFF3* in TNBC.

## 5. Conclusions

*AFF3* expression was significantly downregulated in TNBC tissues and was correlated with malignant status and prognosis. Future studies should examine the regulatory mechanisms of *AFF3*-mediated signaling pathways and confirm the clinical value of *AFF3* levels in TNBC. Downregulated *AFF3* expression may be associated with poor survival. Thus, *AFF3* is a potential therapeutic target for TNBC.

## Abbreviations

*AFF3*, AF4/FMR2 family member 3; AR, Androgen Receptor; BCA, Bicinchoninic acid; BC, Breast cancer; TCGA-BRCA, the Cancer genome atlas-breast invasive carcinoma; BP, Biological process; CC, Cellular components; CDK, Cyclin-dependent kinases; CI, Confidence interval; Cox, Proportional hazards model; DEGs, Differentially expressed genes; DFS, Disease free survival; DNA, Deoxyribo Nucleic Acid; FC, Fold change; FDR, False discovery rate; GEO, Gene Expression Omnibus; GO, Gene Ontology; GSEA, Gene Set Enrichment Analysis; HR, Hazard ratio; KEGG, Kyoto Encyclopedia of Genes and Genomes; L1000FWD, L1000 fireworks display; MF, Molecular Function; MsigDB, Molecular Signatures Database; NES, Normalized enrichment score; OS, Overall survival; PGE2, Prostaglandin E2; qRT-PCR, Quantitative real-time polymerase chain reaction; TCGA, The Cancer Genome Atlas; TICs, Tumor-infiltrating immune cell; TME, Tumor microenvironment; TNBC, triple-negative breast cancer; ER, estrogen receptor; PR, progesterone receptor; HER2, Human Epidermal Growth Factor Receptor 2; TNBC, triple-negative breast cancer; GEO, Gene Expression Omnibus: GEO Platform; GSE, GEO Series.

## Availability of Data and Materials

The datasets used and/or analyzed during the current study are available from the corresponding author on reasonable request.

## Author Contributions

JC, TY and CH contributed to study design/planning. CH, JC and BT contributed to data collection/entry. BT, WZ, TY, JL contributed to data analysis/statistics. CH, JC and JL contributed to data interpretation. CH, JC, and TY contributed to preparation of manuscript. WZ, TY and JL contributed to literature analysis/search. All authors contributed to editorial changes in the manuscript. All authors read and approved the final manuscript. All authors have participated sufficiently in the work to take public responsibility for appropriate portions of the content and agreed to be accountable for all aspects of the work in ensuring that questions related to its accuracy or integrity.

## Ethics Approval and Consent to Participate

The study was performed in accordance with the principles of the Declaration of Helsinki. The study was approved by the Ethics Committee of the Jiangxi Cancer Hospital of Nanchang University (Approval Number: 2021ky227), and all participants provided written informed consent to participate and for publication.

## Acknowledgment

Not applicable.

## Funding

This study was supported by Science and Technology Research Project of Jiangxi Provincial Education Department (Grant Number: GJJ2208202, GJJ2203530).

## Conflict of Interest

The authors declare no conflict of interest.

## Supplementary Material

Supplementary material associated with this article can be found, in the online version, at <https://doi.org/10.31083/j.ceog5008165>.

## References

- [1] Goldhirsch A, Winer EP, Coates AS, Gelber RD, Piccart-Gebhart M, Thürlimann B, *et al.* Personalizing the treatment of women with early breast cancer: highlights of the St Gallen International Expert Consensus on the Primary Therapy of Early Breast Cancer 2013. *Annals of Oncology*. 2013; 24: 2206–2223.
- [2] Zhao Z, Li Y, Liu H, Jain A, Patel PV, Cheng K. Co-delivery of IKBKE siRNA and cabazitaxel by hybrid nanocomplex inhibits invasiveness and growth of triple-negative breast cancer. *Science Advances*. 2020; 6: eabb0616.
- [3] Nair A, Chung HC, Sun T, Tyagi S, Dobrolecki LE, Dominguez-Vidana R, *et al.* Combinatorial inhibition of PTPN12-regulated receptors leads to a broadly effective therapeutic strategy in triple-negative breast cancer. *Natural Medicines*. 2018; 24: 505–511.
- [4] Zhao Y, Wu D, Jiang D, Zhang X, Wu T, Cui J, *et al.* A sequential methodology for the rapid identification and characterization of breast cancer-associated functional SNPs. *Nature Communications*. 2020; 11: 3340.
- [5] Zhang X, Ge X, Jiang T, Yang R, Li S. Research progress on immunotherapy in triple-negative breast cancer (Review). *International Journal of Oncology*. 2022; 61: 95.
- [6] Shi Y, Zhao Y, Zhang Y, AiErken N, Shao N, Ye R, *et al.* *AFF3* upregulation mediates tamoxifen resistance in breast cancers. *Journal of Experimental and Clinical Cancer Research*. 2018; 37: 254.
- [7] Komatsu M, Yoshimaru T, Matsuo T, Kiyotani K, Miyoshi Y, Tanahashi T, *et al.* Molecular features of triple negative breast cancer cells by genome-wide gene expression profiling analysis. *International Journal of Oncology*. 2013; 42: 478–506.
- [8] Boac BM, Abbasi F, Ismail-Khan R, Xiong Y, Siddique A, Park H, *et al.* Expression of the BAD pathway is a marker of triple-negative status and poor outcome. *Scientific Reports*. 2019; 9: 17496.
- [9] Wang L, Shen X, Xie B, Ma Z, Chen X, Cao F. Transcriptional profiling of differentially expressed long non-coding RNAs in breast cancer. *Genomics Data*. 2015; 6: 214–216.
- [10] Weinstein JN, Collisson EA, Mills GB, Shaw KR, Ozenberger BA, Ellrott K, *et al.* The Cancer Genome Atlas Pan-Cancer analysis project. *Nature Genetics*. 2013; 45: 1113–1120.
- [11] Voduc KD, Cheang MC, Tyldesley S, Gelmon K, Nielsen TO, Kennecke H. Breast cancer subtypes and the risk of local and regional relapse. *Journal of Clinical Oncology*. 2010; 28: 1684–1691.
- [12] The Gene Ontology Resource: 20 years and still GOing strong. *Nucleic Acids Research*. 2019; 47: D330–D338.
- [13] Kanehisa M, Furumichi M, Tanabe M, Sato Y, Morishima K. KEGG: new perspectives on genomes, pathways, diseases and drugs. *Nucleic Acids Research*. 2017; 45: D353–D361.
- [14] Mootha VK, Lindgren CM, Eriksson KF, Subramanian A, Sihag S, Lehar J, *et al.* PGC-1 $\alpha$ -responsive genes involved in oxidative phosphorylation are coordinately downregulated in human diabetes. *Nature Genetics*. 2003; 34: 267–273.
- [15] Subramanian A, Tamayo P, Mootha VK, Mukherjee S, Ebert BL, Gillette MA, *et al.* Gene set enrichment analysis: a knowledge-based approach for interpreting genome-wide expression profiles. *Proceedings of the National Academy of Sciences of the United States of America*. 2005; 102: 15545–15550.
- [16] Wang Z, Lachmann A, Keenan AB, Ma'ayan A. L1000FWD: fireworks visualization of drug-induced transcriptomic signatures. *Bioinformatics*. 2018; 34: 2150–2152.
- [17] Gentles AJ, Newman AM, Liu CL, Bratman SV, Feng W, Kim D, *et al.* The prognostic landscape of genes and infiltrating immune cells across human cancers. *Natural Medicines*. 2015; 21: 938–945.
- [18] Lefèvre L, Omeiri H, Drougat L, Hantel C, Giraud M, Val P, *et al.* Combined transcriptome studies identify *AFF3* as a mediator of the oncogenic effects of  $\beta$ -catenin in adrenocortical carcinoma. *Oncogenesis*. 2015; 4: e161.
- [19] To MD, Faseruk SA, Gokgoz N, Pinnaduwa D, Done SJ, Andrulis IL. LAF-4 is aberrantly expressed in human breast cancer. *International Journal of Cancer*. 2005; 115: 568–574.
- [20] Chen F, Li Y, Qin N, Wang F, Du J, Wang C, *et al.* RNA-seq analysis identified hormone-related genes associated with prognosis of triple negative breast cancer. *Journal of Biomedical Research*. 2020; 34: 129–138.
- [21] Weng YS, Tseng HY, Chen YA, Shen PC, Al Haq AT, Chen LM, *et al.* MCT-1/miR-34a/IL-6/IL-6R signaling axis promotes EMT progression, cancer stemness and M2 macrophage polarization in triple-negative breast cancer. *Molecular Cancer*. 2019; 18: 42.
- [22] Ravandi F, Cortes JE, Jones D, Faderl S, Garcia-Manero G, Konopleva MY, *et al.* Phase I/II study of combination therapy with sorafenib, idarubicin, and cytarabine in younger patients with acute myeloid leukemia. *Journal of Clinical Oncology*. 2010; 28: 1856–1862.
- [23] Zhang Y, Li Q, Xu D, Li T, Gu Z, Huang P, *et al.* Idarubicin-induced oxidative stress and apoptosis in cardiomyocytes: An *in vitro* molecular approach. *Human & Experimental Toxicology*. 2021; 40: S553–S562.
- [24] Alamer M, Darbre PD. Effects of exposure to six chemical ultraviolet filters commonly used in personal care products on motility of MCF-7 and MDA-MB-231 human breast cancer cells *in vitro*. *Journal of Applied Toxicology*. 2018; 38: 148–159.
- [25] Burstein MD, Tsimelzon A, Poage GM, Covington KR, Contreras A, Fuqua SA, *et al.* Comprehensive genomic analysis identifies novel subtypes and targets of triple-negative breast cancer. *Clinical Cancer Research*. 2015; 21: 1688–1698.
- [26] Braal CL, Jongbloed EM, Wilting SM, Mathijssen RHJ, Koolen SLW, Jager A. Inhibiting CDK4/6 in Breast Cancer with Palbociclib, Ribociclib, and Abemaciclib: Similarities and Differences. *Drugs*. 2021; 81: 317–331.

- [27] Asghar US, Barr AR, Cutts R, Beaney M, Babina I, Sampath D, *et al.* Single-Cell Dynamics Determines Response to CDK4/6 Inhibition in Triple-Negative Breast Cancer. *Clinical Cancer Research*. 2017; 23: 5561–5572.
- [28] Antoniadou K, Herz C, Le NPK, Mittermeier-Kleßinger VK, Förster N, Zander M, *et al.* Identification of Salicylates in Willow Bark (*Salix Cortex*) for Targeting Peripheral Inflammation. *International Journal of Molecular Sciences*. 2021; 22: 11138.
- [29] Xing L, Yang CX, Zhao D, Shen LJ, Zhou TJ, Bi YY, *et al.* A carrier-free anti-inflammatory platinum (II) self-delivered nanoprodug for enhanced breast cancer therapy. *Journal of Controlled Release*. 2021; 331: 460–471.
- [30] Elwakeel E, Brüggemann M, Wagih J, Lityagina O, Elewa MAF, Han Y, *et al.* Disruption of prostaglandin E2 signaling in cancer-associated fibroblasts limits mammary carcinoma growth but promotes metastasis. *Cancer Research*. 2022; 82: 1380–1395.